IEEE Photonics Journal
An IEEE Photonics Society Publication

Graphene Fabrication by Using Femtosecond Pulsed Laser and Its Application on Passively Q-Switched Solid-State Laser as Saturable Absorber

Volume 12, Number 2, April 2020

Guangying Li
Guodong Zhang
Rui Lou
Yishan Wang
Xiaoping Xie
Jiang Wang
Yonggang Wang
Guanghua Cheng

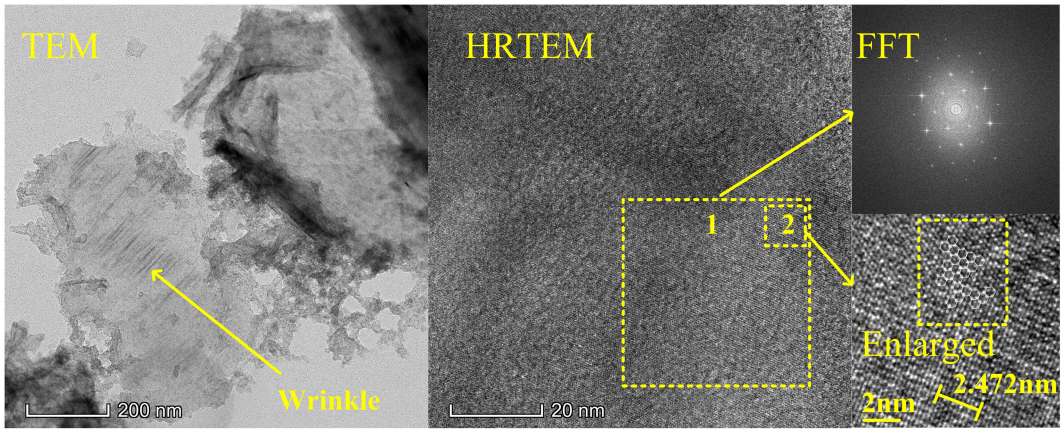

DOI: 10.1109/JPHOT.2020.2966217

IEEE photonics SOCIETY
IEEE

Graphene Fabrication by Using Femtosecond Pulsed Laser and Its Application on Passively Q-Switched Solid-State Laser as Saturable Absorber

Guangying Li,[1,2] **Guodong Zhang**,[1] **Rui Lou**,[1] **Yishan Wang**,[1] **Xiaoping Xie**,[1] **Jiang Wang**,[3] **Yonggang Wang**,[3] **and Guanghua Cheng**[4]

[1]State Key Laboratory of Transient Optics and Photonics, Xi'an Institute of Optics and Precision Mechanics of CAS, Xi'an 710119, China
[2]School of Future Technology, University of Chinese Academy of Sciences, Beijing 100049, China
[3]School of Physics and Information Technology, Shaanxi Normal University, Xi'an 710119, China
[4]Electronic Information College, Northwestern Polytechnical University, Xi'an, Shaanxi 710072, China

DOI:10.1109/JPHOT.2020.2966217

Manuscript received December 1, 2019; revised January 9, 2020; accepted January 9, 2020. Date of publication January 12, 2020; date of current version March 9, 2020. This work was supported in part by the National Natural Science Foundation of China under Grant 61775236 and in part by the National Key Research and Development Program under Grant 2018YFB1107401. Corresponding author: Guanghua Cheng (e-mail: guanghuacheng@nwpu.edu.cn).

Abstract: Here we report on the exfoliation of graphene by using femtosecond pulsed laser with the highly oriented pyrolytic graphite (HOPG) immersed in water. The size of the graphene flakes was demonstrated to be well regulated by controlling the peak-power density of the femtosecond laser irradiation on the HOPG. The transmission electron microscopy (TEM) and Raman spectroscopy were used to identify the morphology and crystalline phase of the graphene. As an application, the few-layers-graphene absorber with a modulation depth of 0.5% was used in a passive Q-switched Nd: YVO_4 laser. A Q-switched nanosecond pulse train with the maximum pulse energy of 262.35 nJ and the narrowest pulse duration of 131.6 ns was obtained.

Index Terms: Femtosecond pulsed laser exfoliation, graphene, Q-switched laser.

1. Introduction

Due to the unique chemical and physical features, graphene which is known as a kind of 2D material has been applied in many fields in past decades. All-optical modulators [1], electro-optical modulators [2], [3], transistors [4], photodetectors [5], electromechanical resonators [6], supercapacitors [7], liquid crystal devices [8], sensors [9] have been demonstrated successfully. Graphene based devices exhibit excellent performance in comparison with traditional devices. For instance, graphene materials prepared with the gas-based hydrazine reduction show a capacitance of 205 F/g and an energy density of 28.5 Wh/kg [10]. The field-effect-transistors made of graphene were demonstrated ultrafast photocurrent response up to 40 GHz [11]. In addition, graphene has

the characteristic of optical saturation absorption (SA) like other materials, for example topological insulator [12], black phosphorus [13] and MXene $Ti_3C_2T_x$ (T = F, O, or OH) [14]. The features of small wavelength dependence [15], low saturation fluence [16] and ultrafast recovery time [17] make graphene an ideal candidate for serving as SA used in laser to produce ultrashort/short pulses and optical solitons [18], [19].

Several methods for fabrication of single/few-layer graphene have been proposed, such as mechanical exfoliation [20], liquid-phase exfoliation [21], chemical vapor deposition [22], molecular beam epitaxy [23]. However, these methods have suffered from several disadvantages. For instance, mechanical exfoliation and liquid exfoliation are time consuming and low yield, while chemical vapor deposition and molecular beam epitaxy need high temperature and high vacuum conditions. Therefore, the production of graphene through a high-yield, time-saving, environmentally-friendly, and one-step method is expected.

Laser-exfoliation graphene provides a method to produce and pattern graphene films. Exfoliation of graphene by using nanosecond pulsed laser and continuous wave (CW) CO_2 laser have been reported [24]–[26]. Long pulse and CW laser-exfoliation formation is more likely to be caused by photothermal effects. Photothermal effect induces plenty of defects in the process of laser ablation [27]. Femtosecond pulsed laser has attracted considerable attention in the micro-nano processing for the characteristic of quasi-nonthermal processing [28]–[30]. The femtosecond laser exfoliation is therefore expected to show the capability for producing defects-free monolayer graphene. However, there are few reports on the femtosecond laser exfoliation. And the crystallinity and quality of the exfoliated graphene are not good enough. The exfoliation process is urgently necessary to be optimized. The behaviors and further applications of the femtosecond-laser-exfoliated graphene remain to be carefully studied.

In this work, graphene was demonstrated to be directly exfoliated from bulk HOPG by using femtosecond pulsed laser with a repetition rate of 100 kHz. The average size of the graphene flakes can be well regulated by controlling the peak intensity of the laser irradiation. Then the laser-exfoliated graphene was used as SA in a passive Q-switched laser. A Q-switched nanosecond pulse train was obtained with the maximum pulse energy of 262.35 nJ and the narrowest pulse duration of 131.6 ns.

2. Experimental Setup

2.1 Preparation and Characterization of Graphene

A bulk HOPG ($5 \times 5 \times 1$ mm^3, Grade B, XFNANO, Inc) was immersed in the deionized water in a quartz vessel, which was fixed on the three-dimensional stages (ANT130, Aerotech). The schematic diagram is shown in Fig. 1. The femtosecond pulsed laser (Pharos, Lightconversion) with pulse duration of 225 fs and wavelength of 1030 nm was utilized to irradiate the bulk HOPG at a frequency of 100 kHz and pulse energy of 8 μJ. A 20$\times$ objective lens was used to focus the laser on the HOPG sample with a radius of 1 μm. Accordingly, its peak power density is up to 1.132×10^{15} W/cm^2. The speed of the three-dimensional moving platform was fixed at 100 μm/s. Abundant up-floating flakes could be seen in the observation system during the laser irradiation, at the same time, the solution gradually changed into the grey color. After laser exfoliation, the supernatant was collected into a glass bottle and kept for 24 hours to obtain the few-layers graphene. Then the few-layers graphene solution was injected into a 0.5 mm thickness quartz cell which was coated to antireflective at 1064 nm. Finally, the quartz cell with laser-exfoliated graphene solution acted as a transmission-type absorber for the Q-switched laser operation.

The laser-exfoliated graphene solution was dropped on the monocrystalline silicon and characterized by Raman spectroscopy which excited by a 532 nm laser source. The spectrum was showed in Fig. 2(a). Curve 1 shows the Raman spectrum of HOPG, which displayed a G-band at 1580 cm^{-1} and a broad doublet structure 2D-band at 2718 cm^{-1}, the D-band at about 1350 cm^{-1} are absent comparing to graphene, which has three peaks at 1347 cm^{-1}, 1587 cm^{-1}, 2700 cm^{-1} correspond to D-band, G-band, 2D-band, respectively. The G peak corresponds to the E_{2g} phonon

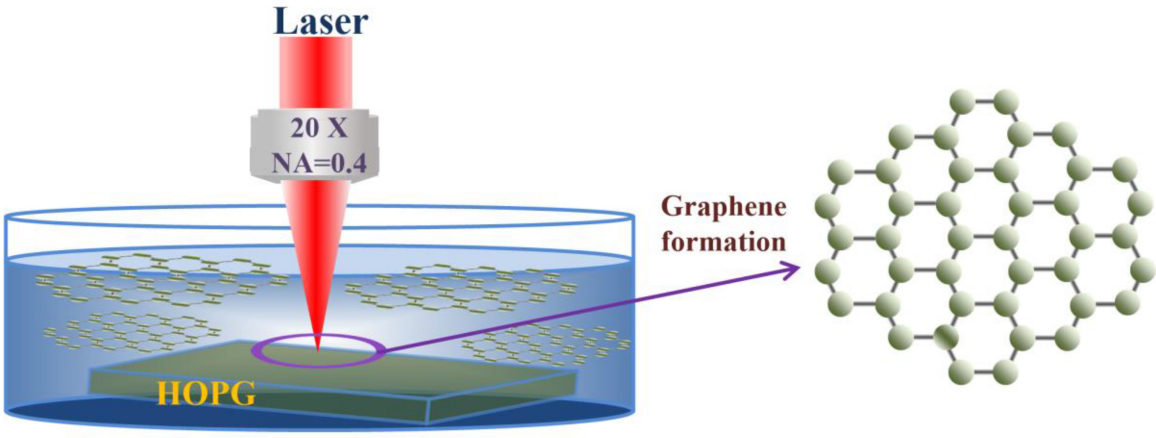

Fig. 1. Experimental setup for laser exfoliation of bulk HOPG.

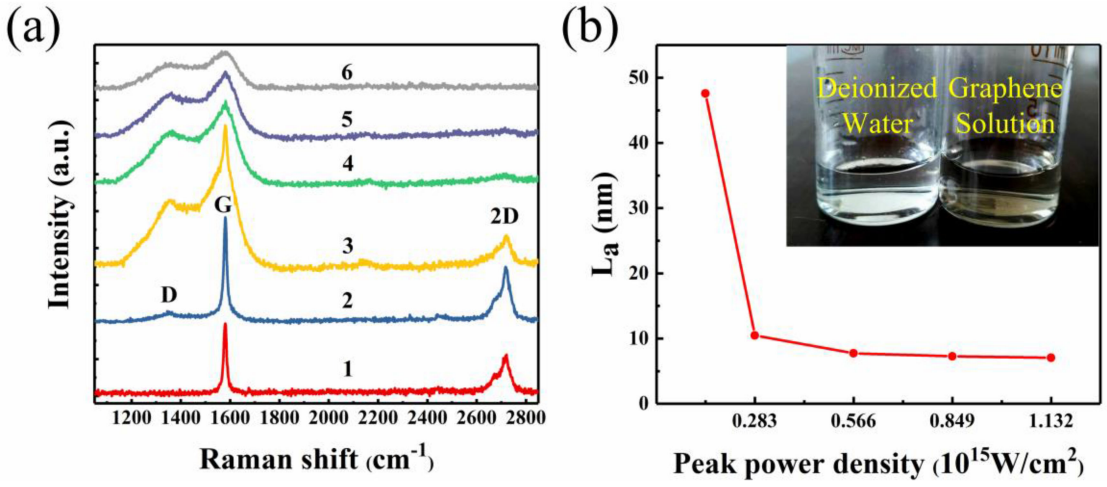

Fig. 2. (a) Raman spectrum of the sample: 1, the HOPG; 2, exfoliated graphene at 0.1415 $\times$ 10^{15} W/cm^2; 3, exfoliated graphene at 0.283 $\times$ 10^{15} W/cm^2; 4, exfoliated graphene at 0.566 $\times$ 10^{15} W/cm^2; 5, exfoliated graphene at 0.849 $\times$ 10^{15} W/cm^2; 6, exfoliated graphene at 1.132 $\times$ 10^{15} W/cm^2. (b) The L_a versus peak power density. The inset is the image of the prepared graphene solutions and deionized water.

at the Brillouin zone center, the D peak is due to the breathing modes of sp^2 rings and requires a defect for its activation by double resonance, the 2D peak is the second order of the D peak [31]. The Raman spectra of the graphene exfoliated by femtosecond laser with different peak power densities are shown as curve 2- curve 6 in Fig. 2(a). Different from that of the HOPG, the D band at about 1350 cm^{-1} appears in the Raman spectrum of the laser-exfoliated graphene, moreover, the D-band and G-band are broadened, which indicate that the exfoliated graphene was in a few-layers form [32].

The average size of the graphene flakes can be theoretically estimated by using the well-known Tuinstra-Koenig (T-K) equation $L_a = C(\lambda)/(I_D/I_G)$ [33], where I_D and I_G are the intensity of D band and G band, respectively. The $C(\lambda)$ is a constant which is related to the excitation wavelength of Raman spectroscopy, in our case, $C(\lambda)$ is ~49.56 Å [34]. The L_a represents the average size of graphene. The red line in Fig. 2(b) shows the values of L_a with varying peak power density of laser irradiation ranging from 0.1415 $\times$ 10^{15} to 1.132 $\times$ 10^{15} W/cm^2. It can be obtained that the exfoliated graphene has a nanometer-scale size ranging from 47.6 nm to 7 nm. The average size

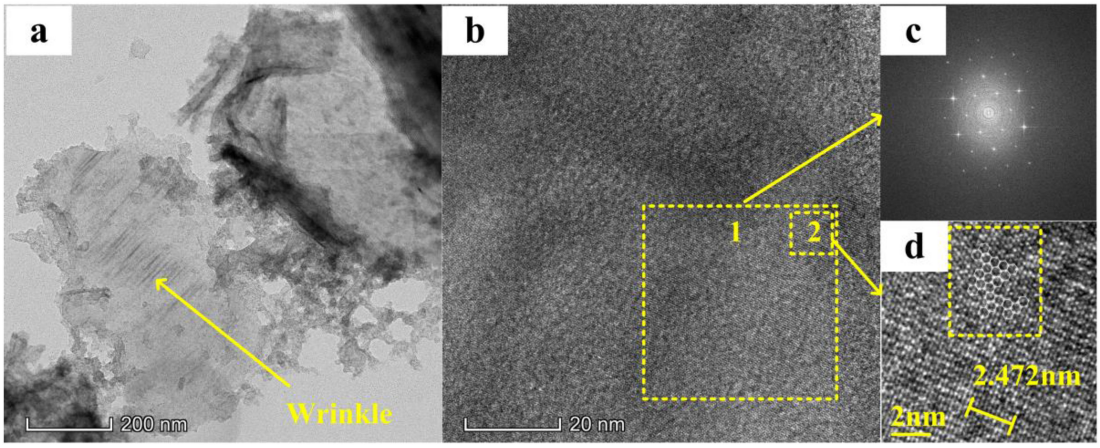

Fig. 3. (a) TEM image of curled graphene at low magnification. (b) Lattice-resolved HRTEM image of graphene. (c) FFT pattern of region 1. (d) Enlarged view of region 2.

decreases with the increase of peak power density. The inset in Fig. 2(b) demonstrates the images of prepared graphene solutions and deionized water. The physical nature of the laser exfoliation can be concluded that the shock wave induced and propagated on HOPG interface overcome the van der Waals forces between adjacent graphene layers [35]. The van der Waals force is estimated to be only 2.6×10^{-4} eV [36] which is much smaller than the C-C bond strength (3.7 eV). Therefore, the shock-wave induced at low peak power density is enough for the exfoliation. When the peak power density is further increased, surface ablation and intense shock wave will be triggered which will reduce crystallinity and fragment the exfoliated grapheme.

The transmission electron microscopy (TEM) was used to characterize the morphology and structure of the exfoliated graphene under peak power density of 0.1415×10^{15} W/cm^2, for which the graphene sheets are considered to be in the largest averaged size. Fig. 3(a) shows the image of two pieces of exfoliated graphene flakes which are respectively in the size of 760×480 nm^2 and 910×480 nm^2 with wrinkled morphologies. High-resolution TEM image presents a perfect crystalline structure of the graphene sheets as shown in Fig. 3(b). A fast Fourier transformation (FFT) of region 1 in Fig. 3(b) results in a hexagonal pattern as shown in Fig. 3(c), revealing the six-fold symmetry feature of graphene. The hexagonal arrangement of carbon rings can be identified from Fig. 3(d), which is an enlarged view of region 2, and the d-spacing of the graphene is measured to be 2.472 Å which is consistent with the value reported by S.Z. Mortazavi [26].

Considering the characterization results above, we chose the graphene exfoliated at peak power density of 0.1415×10^{15} W/cm^2 as the saturable absorber for its larger size. The linear transmission of the laser-exfoliated graphene solution at a wavelength ranging from 300 nm to 1100 nm was characterized by using a spectrophotometer. The result is depicted in Fig. 4(a). It could be seen that the transmission of the graphene solution is about 88.5% at the laser wavelength of 1030 nm.

Furthermore, we investigated the nonlinear optical absorption property of the laser-exfoliated graphene solution. Balanced twin-detector measurement technique was adopted [37]. The inset in Fig. 4(b) shows the schematic diagram. The femtosecond pulsed laser with a repetition rate of 10 kHz, a central wavelength of 1030 nm and pulse duration of 225 fs was used as the laser source for the characterization. The laser beam was split into two arms with equal power by 50/50 beamsplitter. One arm was used for power-dependent transmission measurement of SA and the other one as a reference. The input power was controlled by variable optical attenuator. By continuously adjusting the incident power, the twin-detector power meter records the relationship between the output power and the input power. Consequently, the transmittance of graphene solution under different irradiation condition was obtained as shown in Fig. 4(b).The experimental

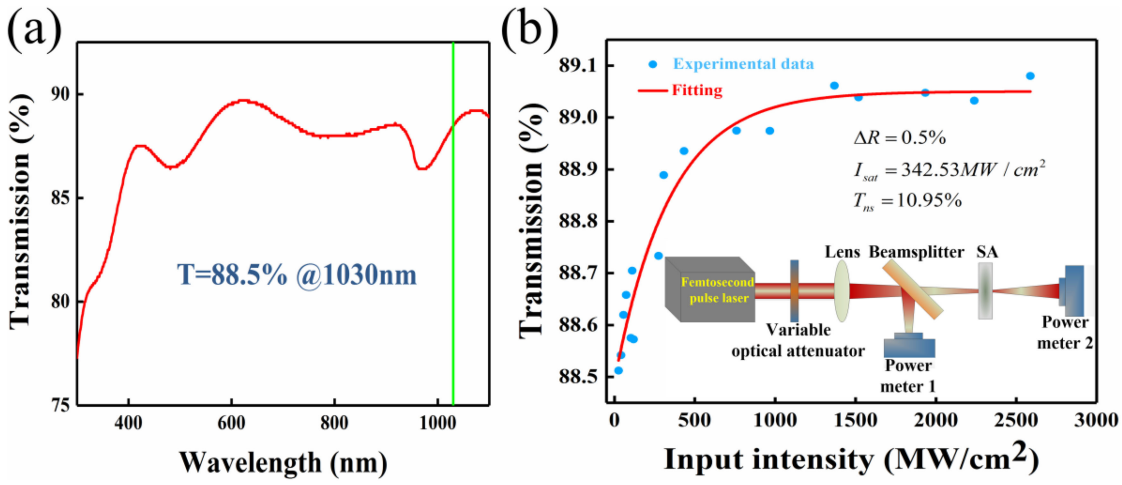

Fig. 4. (a) The linear optical transmission curve of the graphene SA. (b) The nonlinear optical transmission curve of the graphene SA.

results were further fitted by the following formula [38]:

$$T(I) = 1 - \Delta T \times \exp(-I/I_{sat}) - T_{ns} \quad (1)$$

Where $T(I)$ is the transmission, ΔT is the modulation depth, I is the input intensity, I_{sat} is the saturation intensity, and T_{ns} is the non-saturable loss. Based on the fitting results, we can conclude that the modulation depth (ΔT), saturable intensity (I_{sat}), and non-saturable loss (T_{ns}) are 0.5%, 342.53 MW/cm^2, and 10.95%, respectively. The above shows that the graphene exfoliation by femtosecond pulse laser is an easy-to-implement and environmentally-friendly approach to generate graphene. One-step fabrication process without high vacuum and high temperatures devices and additional chemical components is a prominent advantage. The fabrication process could be controllable by changing the laser properties and the irradiation conditions. Furthermore, the graphene exfoliated could put into application directly.

2.2 Passively Q-Switched Operation by Graphene

A linear cavity was used for investigating passively Q-switched solid-state laser with laser-exfoliated graphene solution as SA. The experimental setup is illustrated in Fig. 5. A 12-W fiber-coupled laser diode (LD) with wavelength centered at 808 nm is used as the pump source. The core diameter and numerical aperture of the output fiber of the laser diode were 100 μm and 0.22, respectively. The pump laser was focused on the gain crystal with a focus diameter of 200 μm. A $3 \times 3 \times 5$ mm^3 Nd: YVO_4 crystal with Nd^{3+} concentration of 0.5% was employed as the gain medium. The side of the crystal towards the pump laser was antireflective at 808 nm and highly reflective at 1064 nm. The other side was antireflective both at 808 nm and 1064 nm. The Nd: YVO_4 crystal was wrapped with indium foil and mounted in a water-cooled copper block which was kept at the temperature of 20 °C. The SA was inserted into the cavity close to the output coupler (OC). In order to avoid the thermal instability of graphene SA for high power density in the cavity, output coupler of T = 70% and T = 80% were adopted.

3. Experimental Results and Discussions

When the slant angle of graphene SA in the laser cavity was adjusted carefully and the pump power was increased gradually, the Q-switched laser operation could be setup. The average output power versus incident pump power (P_{in}) in Q-switched operation under output coupler of T = 70% and

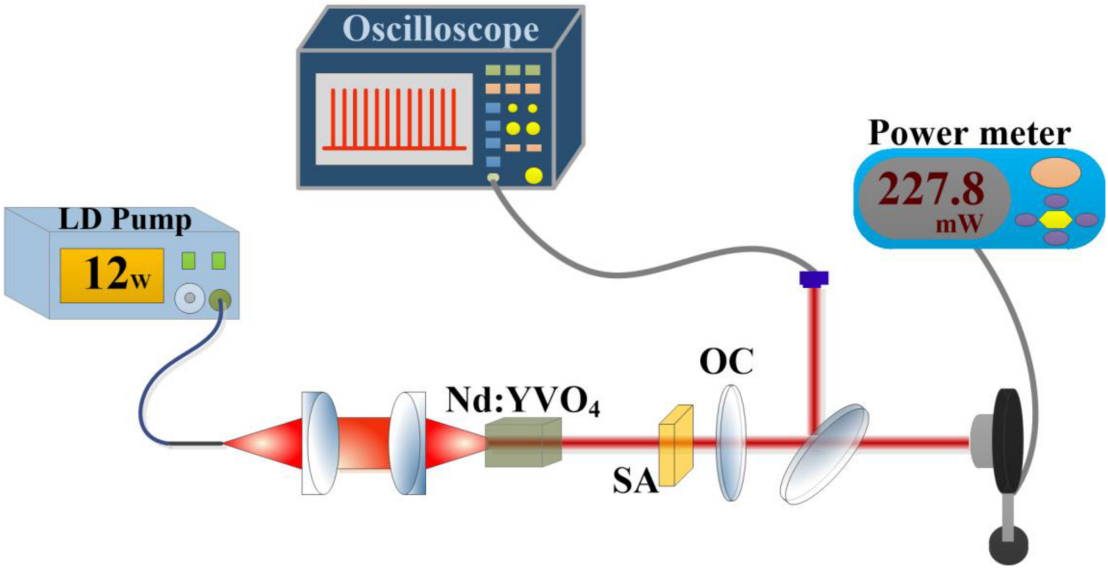

Fig. 5. Schematic experimental setup of passively Q-switched laser with graphene SA.

T = 80% are explored and described in Fig. 6(a). The average output power almost linearly increases with the increase of incident pump power. The highest output power is 227.8 mW and 173.8 mW with output coupler of T = 70% and T = 80%, respectively. The relatively low output power is due to the high output coupling and high non-saturable loss of the graphene SA. The output pulse trains were recorded by an oscilloscope with 200 MHz bandwidth and a fast InGaAs photodetector with a rise time of 70 ps.

The dependence of pulse duration and repetition rate on incident pump power for the output coupler of T = 70% and T = 80% are recorded in Fig. 6(b). With the increase of incident pump power, the repetition rate elevates, whereas the pulse duration decreases. For the case of output coupler T = 70%, the threshold of incident pump power for the Q-switched operation is 5.94 W. With further increasing the incident pump power from 5.94 W to 8.57 W, the repetition rate quasi-linear increases from 277.8 kHz to 868.3 kHz, meanwhile, the pulse duration monotonously decreases from 346 ns to 131.6 ns. For the case of output coupler T = 80%, the threshold of incident pump power for the Q-switched operation is 6.34 W. With further increasing the incident pump power from 6.34 W to 8.57 W, the repetition rate increases from 281.9 kHz to 842.5 kHz, meanwhile, the pulse duration monotonously decreases from 413.5 ns to 185.2 ns. Therefore, we obtain that the shortest pulse duration for output coupler of T = 70% and T = 80% are 136.1 ns and 185.2 ns, respectively. The influence of incident pump power on the pulse train for output coupler of T = 70% and T = 80% can be also intuitively observed in Fig. 6(c) and Fig. 6(d). The insets in Fig. 6(c) and Fig. 6(d) show the temporal profile of the shortest pulse for output coupler of T = 70% and T = 80%, respectively. Note that, when the incident pump power is further increased to be above 8.57 W, the pulse train will become chaotic and irregular. The output power instability (rms) of the Q-switched laser is measured to be 3.5% for 12 hours. In the end, the maximum pulse energy of 262.35 nJ and the narrowest pulse duration of 131.6 ns was obtained. Table 1 summarizes the results obtained from passive Q-switched lasers based on graphene SA. Compared to other previously reported values, narrower pulse width was obtained with small modulation depth.

The output spectra of the Q-switched laser with graphene SA and the CW laser without graphene SA were shown in Fig. 7(a) and Fig. 7(b). The output spectra were measured by a spectrograph with measuring accuracy of 0.02 nm. For the Q-switched laser with graphene SA, the central wavelength locates at 1064.41 nm with a bandwidth of 0.16 nm under the output coupler of T = 70% and the central wavelength locates at 1064.50 nm with a bandwidth of 0.20 nm under the output coupler of

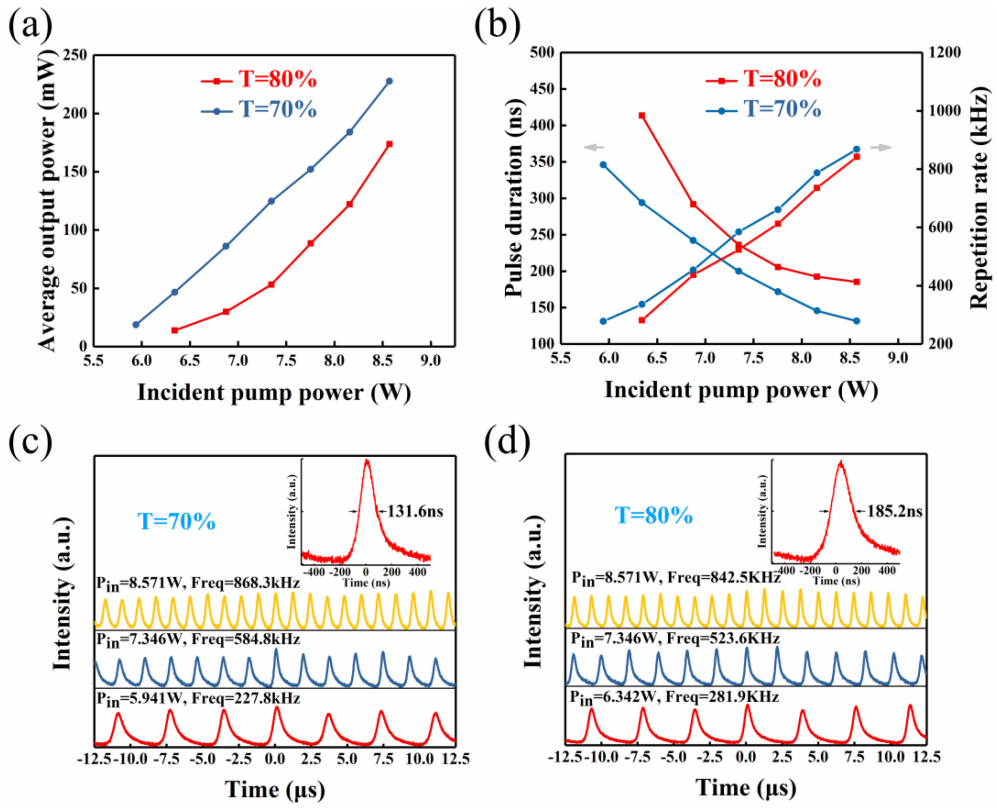

Fig. 6. (a) The average output power versus incident pump power. (b) The pulse duration and the pulse repetition rate versus incident pump power. (c) The pulse train under different incident pump power at output coupling of T = 70%. (d) The pulse train under different incident pump power at output coupling of T = 80%. The inset shows the temporal profile of a single pulse.

TABLE 1
Comparison of Laser Result Based on Graphene-SA

Laser type	MD(%)	τ(ns)	P(mW)	Frep(kHz)	Ref.
Tm:CLNGG	1	9000	40	5.8	[39]
Nd:$GdVO_4$	4.5	450	260	43	[40]
Nd:YAG	6	161	105	660	[41]
Ho:YVO_4	10	265.2	2200	131.6	[42]
Yb:YAG	-	228	185	285	[43]
Nd:YAG	-	400	575	850	[44]
Yb:KYW	-	349	34	607	[45]
Nd:YVO_4	0.5	131.6	227.8	868.3	Our work

MD, modulation depth; τ, pulse duration; P, average output power; Frep, repetition frequency.

T = 80%. However, for the CW laser, the central wavelength locates at 1064.44 nm and 1064.52 nm with a bandwidth of 0.17 nm and 0.22 nm under the output coupler of T = 70% and T = 80%. The change of laser central wavelength and the bandwidth was considered to be influenced by the temperature of laser crystal. The inset shown in Fig. 7(a) is the beam profile, which was measured with a charge-coupled device (CCD) camera at the highest-power output of 227.8 mW, indicating

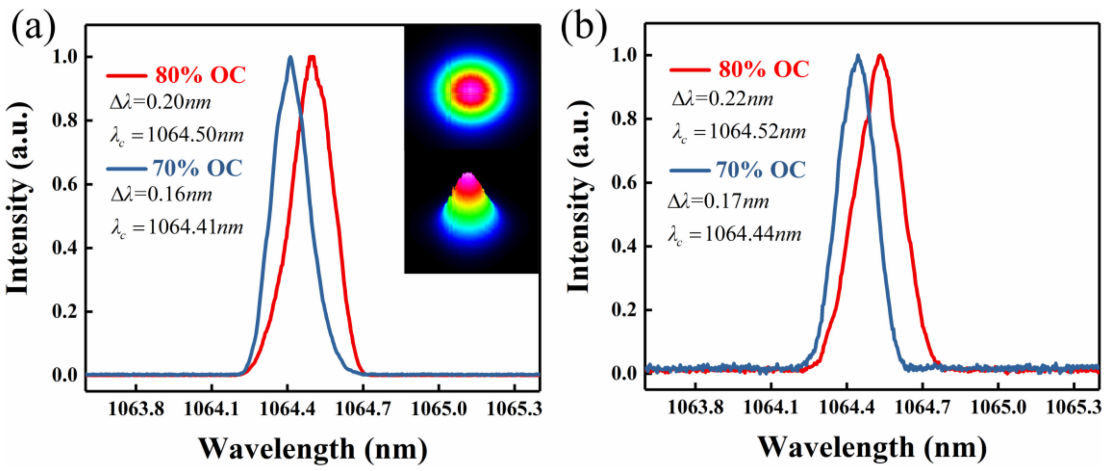

Fig. 7. (a) The output spectra of Q-switched laser with graphene SA. The inset shows the beam profile. (b) The output spectra of CW laser without graphene SA.

a perfect TEM_{00} mode. The beam quality factor of $M_x^2 = 1.8594$, $M_y^2 = 1.9487$ are calculated at two directions perpendicular to the axis of laser propagation.

4. Conclusion

In this paper, we fabricated the few-layers graphene by using the highly oriented pyrolytic graphite (HOPG) through the femtosecond laser exfoliation. The average size of the graphene flakes was proved to be able to be regulated by controlling the peak-power density of the femtosecond laser irradiation. The TEM and Raman characterization indicated that the exfoliated graphene had a good morphology and crystalline phase. The graphene exfoliated at peak power density of 0.1415×10^{15} W/cm^2 was characterized to have a modulation depth of 0.5% for 1030 nm femtosecond laser. Furthermore, the graphene dispersed in the deionized water was applied in the passive Q-switched laser as the SA. A Q-switched nanosecond pulse train with the maximum pulse energy of 262.35 nJ and the narrowest pulse duration of 131.6 ns was obtained. Femtosecond laser exfoliation provides a flexible and powerful way for fabrication of graphene.

References

[1] W. Li *et al.*, "Ultrafast all-optical graphene modulator," *Nano Lett.*, vol. 14, no. 2, pp. 955–959, 2014.
[2] C. C. Lee, S. Suzuki, W. Xie, and T. R. Schibli, "Broadband graphene electro-optic modulators with sub-wavelength thickness," *Opt. Express*, vol. 20, no. 5, pp. 5264–5269, 2012.
[3] J. Bogusławski *et al.*, "Graphene actively mode-locked lasers," *Adv. Funct. Mater.*, vol. 28, no. 28, 2018, Art. no. 1801539.
[4] F. Schwierz, "Graphene transistors," *Nat. Nanotechnol.*, vol. 5, no. 7, p. 487, 2010.
[5] T. Mueller, F. Xia, and P. Avouris, "Graphene photodetectors for high-speed optical communications," *Nat. Photon.*, vol. 4, no. 5, p. 297, 2010.
[6] J. S. Bunch *et al.*, "Electromechanical resonators from graphene sheets," *Science*, vol. 315, no. 5811, pp. 490–493, 2007.
[7] C. Liu, Z. Yu, D. Neff, A. Zhamu, and B. Z. Jang, "Graphene-based supercapacitor with an ultrahigh energy density," *Nano Lett.*, vol. 10, no. 12, pp. 4863–4868, 2010.
[8] P. Blake *et al.*, "Graphene-based liquid crystal device," *Nano Lett.*, vol. 8, no. 6, pp. 1704–1708, 2008.
[9] Z. Cheng, Q. Li, Z. Li, Q. Zhou, and Y. Fang, "Suspended graphene sensors with improved signal and reduced noise," *Nano Lett.*, vol. 10, no. 5, pp. 1864–1868, 2010.
[10] Y. Wang, Z. Shi, Y. Huang, Y. Ma, C. Wang, M. Chen, and Y. Chen, "Supercapacitor devices based on graphene materials," *J. Phys. Chem. C.*, vol. 113, no. 30, pp. 13103–13107, 2009.
[11] F. Xia, T. Mueller, Y.-m. Lin, A. Valdes-Garcia, and P. Avouris, "Ultrafast graphene photodetector," *Nat. Nanotechnol.*, vol. 4, no. 12, p. 839, 2009.

[12] Y. Chen *et al.*, "Large energy, wavelength widely tunable, topological insulator Q-switched erbium-doped fiber laser," *IEEE J. Sel. Top. Quantum Electron.*, vol. 20, no. 5, pp. 315–322, Sep./Oct. 2014.
[13] J. Ma *et al.*, "Few-layer black phosphorus based saturable absorber mirror for pulsed solid-state lasers," *Opt. Express*, vol. 23, no. 17, pp. 22643–22648, 2015.
[14] X. Jiang *et al.*, "Broadband nonlinear photonics in few-layer MXene $Ti_3C_2T_x$ (T = F, O, or OH)," *Laser Photon. Rev.*, vol. 12, no. 2, 2018, Art. no. 1700229.
[15] J. Xu *et al.*, "Performance of large-area few-layer graphene saturable absorber in femtosecond bulk laser," *Appl. Phys. Lett.*, vol. 99, no. 26, 2011, Art. no. 261107.
[16] Q. Bao *et al.*, "Atomic layer graphene as saturable absorber for ultrafast pulsed lasers," *Adv. Funct. Mater.*, vol. 19, no. 19, pp. 3077–3083, 2010.
[17] Z. Wang, Y. Chen, C. Zhao, H. Zhang, and S. Wen, "Switchable dual-wavelength synchronously Q-switched erbium-doped fiber laser based on graphene saturable absorber," *IEEE Photon. J.*, vol. 4, no. 3, pp. 869–876, Jun. 2012.
[18] L. Zhao, D. Tang, X. Wu, and H. Zhang, "Dissipative soliton generation in Yb-fiber laser with an invisible intracavity bandpass filter," *Opt. Lett.*, vol. 35, no. 16, pp. 2756–2758, 2010.
[19] Y. Song, X. Shi, C. Wu, D. Tang, and H. Zhang, "Recent progress of study on optical solitons in fiber lasers," *Appl. Phys. Rev.*, vol. 6, no. 2, 2019, Art. no. 021313.
[20] A. Martinez, K. Fuse, and S. Yamashita, "Mechanical exfoliation of graphene for the passive mode-locking of fiber lasers," *Appl. Phys. Lett.*, vol. 99, no. 12, 2011, Art. no. 121107.
[21] Y. Hernandez *et al.*, "High-yield production of graphene by liquid-phase exfoliation of graphite," *Nat. Nanotechnol.*, vol. 3, no. 9, pp. 563–568, 2008.
[22] S. Das and J. Drucker, "Nucleation and growth of single layer graphene on electrodeposited Cu by cold wall chemical vapor deposition," *Nanotechnology*, vol. 28, no. 10, 2017, Art. no. 105601.
[23] E. Moreau, F. J. Ferrer, D. Vignaud, S. Godey, and X. Wallart, "Graphene growth by molecular beam epitaxy using a solid carbon source," *Phys. Status Solidi A.*, vol. 207, no. 2, pp. 300–303, 2010.
[24] M. An, J. Wu, P. Wang, and Y. Fang, "Double-emission mechanism of laser-induced HOPG-exfoliated Graphene Quantum Dots (GQDs)," *Appl. Phys. Lett.*, vol. 114, no. 2, 2019, Art. no. 022102.
[25] J. Lin *et al.*, "Laser-induced porous graphene films from commercial polymers," *Nat. Commun.*, vol. 5, 2014, Art. no. 5714.
[26] S. Z. Mortazavi, P. Parvin, and A. Reyhani, "Fabrication of graphene based on Q-switched Nd: YAG laser ablation of graphite target in liquid nitrogen," *Laser Phys. Lett.*, vol. 9, no. 7, 2012, Art. no. 547.
[27] S.-J. An, Y. H. Kim, C. Lee, D. Y. Park, and M. S. Jeong, "Exfoliation of transition metal dichalcogenides by a High-Power femtosecond laser," *Sci. Rep.*, vol. 8, no. 1, 2018, Art. no. 12957.
[28] P. Russo, A. Hu, G. Compagnini, W. W. Duley, and N. Y. Zhou, "Femtosecond laser ablation of highly oriented pyrolytic graphite: a green route for large-scale production of porous graphene and graphene quantum dots," *Nanoscale*, vol. 6, no. 4, pp. 2381–2389, 2014.
[29] M. Reininghaus, D. Wortmann, J. Finger, O. Faley, R. Poprawe, and C. Stampfer, "Laser induced non-thermal deposition of ultrathin graphite," *Appl. Phys. Lett.*, vol. 100, no. 15, 2012, Art. no. 151606.
[30] Y. Miyamoto, H. Zhang, and D. Tomanek, "Photoexfoliation of graphene from graphite: An Ab initio study," *Phys. Rev. Lett.*, vol. 104, no. 20, 2010, Art. no. 208302.
[31] Z. Sun *et al.*, "Graphene mode-locked ultrafast laser," *ACS Nano.*, vol. 4, no. 2, pp. 803–810, 2010.
[32] P. Feng, N. Zhang, H. Wu, and X. Zhu, "Effect of ambient air on femtosecond laser ablation of highly oriented pyrolytic graphite," *Opt. Lett.*, vol. 40, no. 1, pp. 17–20, 2015.
[33] A. Ferrari, "Raman spectroscopy of graphene and graphite: Disorder, electron–phonon coupling, doping and nonadiabatic effects," *Solid State Commun.*, vol. 143, no. 1, pp. 47–57, 2007.
[34] M. Matthews, M. Pimenta, G. Dresselhaus, M. Dresselhaus, and M. Endo, "Origin of dispersive effects of the Raman D band in carbon materials," *Phys. Rev. B.*, vol. 59, no. 10, 1999, Art. no. R6585.
[35] G. Compagnini, P. Russo, F. Tomarchio, O. Puglisi, L. D'Urso, and S. Scalese, "Laser assisted green synthesis of free standing reduced graphene oxides at the water–air interface," *Nanotechnology*, vol. 23, no. 50, 2012, Art. no. 505601.
[36] K. H. Michel and B. Verberck, "Theory of the evolution of phonon spectra and elastic constants from graphene to graphite," *Phys. Rev. B.*, vol. 78, no. 8, 2008.
[37] K. Wang *et al.*, "Passively Q-switched laser at 1.3 μm with few-layered MoS_2 saturable absorber," *IEEE J. Select. Top. Quantum Electron.*, vol. 23, no. 1, pp. 71–75, Jan./Feb. 2017.
[38] X. Wang *et al.*, "Titanium dioxide Langmuir–Blodgett film saturable absorber for passively Q-switched Nd: GdVO 4 laser," *IEEE Photon. J.*, vol. 11, no. 2, pp. 1–10, Apr. 2019.
[39] G. Xie *et al.*, "Graphene saturable absorber for Q-switching and mode locking at 2 μm wavelength," *Opt. Mater. Express*, vol. 2, no. 6, pp. 878–883, 2012.
[40] J. Xu *et al.*, "Efficient graphene Q switching and mode locking of 1.34 μm neodymium lasers," *Opt. Lett.*, vol. 37, no. 13, pp. 2652–2654, 2012.
[41] X. Li, J. Xu, Y. Wu, J. He, and X. Hao, "Large energy laser pulses with high repetition rate by graphene Q-switched solid-state laser," *Opt. Exp.*, vol. 19, no. 10, pp. 9950–9955, 2011.
[42] W. Lin, X. Duan, Z. Cui, B. Yao, T. Dai, and X. Li, "A passively Q-switched Ho: YVO_4 Laser at 2.05 μm with Graphene saturable absorber," *Appl. Sci.*, vol. 6, no. 5, p. 128, 2016.
[43] J. M. Serres *et al.*, "Graphene Q-switched compact Yb: YAG laser," *IEEE Photon. J.*, vol. 7, no. 5, pp. 1–7, Oct. 2015.
[44] Q. Wang, Z. Wei, J. Lin, Y. Zhang, L. Guo, and Z. Zhang, "Few-layer graphene as saturable absorber for Q-switched laser at sub-MHz repetition rate," in *Advances in Optical Materials*, Washington, DC, United States: Optical Society of America, 2011, p. AIThF3.
[45] J. W. Kim *et al.*, "Graphene Q-switched Yb: KYW planar waveguide laser," *AIP Adv.*, vol. 5, no. 1, 2015, Art. no. 017110.